Mapping Potential Risk of Rift Valley Fever Outbreaks in African Savannas Using Vegetation Index Time Series Data

Assaf Anyamba, Kenneth J. Linthicum, Robert Mahoney, Compton J. Tucker, and Patrick W. Kelley

Abstract

Rift Valley fever (RVF) outbreaks in East Africa are closely coupled with above normal rainfall that is associated with the occurrence of the warm phase of the El Niño/Southern Oscillation (ENSO) phenomenon. Outbreaks elsewhere in central and southern Africa are also linked to elevated rainfall patterns. Major RVF activity has been reported to occur throughout much of sub-Saharan Africa, except in areas with extensive tropical forest. In this study we used normalized difference vegetation index (NDVI) time-series data derived from the Advanced Very High Resolution Radiometer (AVHRR) instrument on polar orbiting National Oceanographic and Atmospheric Administration (NOAA) satellites to map areas with a potential for an RVF outbreak. A 19-year NDVI climatology was created and used to discriminate between areas with tropical forest, savanna, and desert. Because most RVF outbreaks have occurred in regions dominated by savanna vegetation, we created a mask to identify those areas where RVF would likely occur within the savanna ecosystems. NDVI anomalies were then calculated for the entire time series from July 1981 to the July 2000. Subsequently, we developed a methodology that detects areas with persistent positive NDVI anomalies (greater than + 0.1 NDVI units) using a three-month moving window to flag regions at greatest risk. Algorithms were designed to account for periods of extended above normal NDVI (by inference rainfall) and to consider the complex life cycle of mosquitoes that maintain and transmit RVF virus to domestic animals and people. We present results for different ENSO warm- and cold-event periods. The results indicate that regions of potential outbreaks have occurred predominantly during warm ENSO events in East Africa and during cold ENSO events in southern Africa. Results provide a likely historical reconstruction of areas where RVF may have occurred during the last 19 years. There is a close agreement between confirmed outbreaks between 1981 and 2000, particularly in East Africa, and the risk maps produced in this study. This technique is adaptable to near real-time monitoring on a monthly basis and may be a useful tool in RVF disease surveillance.

Introduction

Rift Valley fever (RVF) is an arthropod-borne viral disease that affects domestic animals and humans. The first documented epizootic of RVF occurred on a farm in 1930–1931 near Lake Naivasha, Kenya with high mortality among sheep (Daubney *et al.*, 1931). The name Rift Valley refers to the location of the first isolation of the virus in the Rift Valley region of Kenya dominated by savanna grasslands. Their findings showed that the disease was vector borne, transmitted by a variety of mosquito species, and affected both domestic animals and humans. The disease is now known to occur periodically over much of sub-Saharan Africa with reported outbreaks in a number of countries including Kenya, Somalia, Egypt, South Africa, Senegal, Mauritania, and Zimbabwe, with RVF activity reported in 25 African countries (Megan and Bailey, 1989; Peters and Linthicum, 1994). The disease results in high mortality and abortions in domestic animals, and a mortality rate of less than 1 percent among humans (Peters and Linthicum, 1994). A recent outbreak in Saudi Arabia and Yemen, (September through November 2000) documents for the first time the occurrence of the RVF virus outside of continental Africa (WHO, 2000).

RVF outbreaks in Kenya (Davies *et al.*, 1985), South Africa (McIntosh and Jupp, 1981), Zambia (Davies *et al.*, 1992), and Zimbabwe (Swanepoel, 1981) have occurred following periods of exceptionally above normal rainfall, with most large-scale epizootic clustering around years of persistent above normal rainfall. Environmentally, outbreaks have occurred in a wide range of ecological zones. In eastern and southern Africa, RVF activity has been reported in the proximity of grassland depressions known as dambos, which seasonally flood and are known to be good habitats for the breeding of *Aedes* and *Culex* mosquito species, which serve as vectors (Linthicum *et al.*, 1983; Linthicum *et al.*, 1984). In dry areas of the Sahel and North Africa, outbreaks are centered around flooded riverine environments and irrigated areas as occurred in Egypt, Senegal, and Mauritania (Peters and Megan, 1981; Wilson *et al.*, 1994, Linthicum *et al.*, 1994). The virus is common among domestic sheep and cattle that graze in bushed and wooded grasslands, with secondary transmission to humans by mos-

A. Anyamba is with the Goddard Earth Sciences Technology Center (GEST)/UMBC, NASA/GSFC, Code 923.0, Greenbelt, MD 20771 (assaf@itpmail.gsfc.nasa.gov).

K.J. Linthicum and P.W. Kelley are with the Department of Defense—Global Emerging Infections System, Walter Reed Army Institute of Research, 503 Robert Grant Avenue, Silver Spring, MD 20910-7500.

K.J. Linthicum is currently with the Vector-Borne Disease Section, California Department of Health Sciences, 2151 Convention Center Way, Ontario, CA 91764.

R. Mahoney is with Global Science and Technology, 6411 Ivy Lane, Greenbelt, MD 20770.

C.J. Tucker is with the NASA/Goddard Space Flight Center, Biospheric Sciences Branch, Code 923.0, Greenbelt, MD. 20771.

Photogrammetric Engineering & Remote Sensing
Vol. 68, No. 2, February 2002, pp. 137–145.

0099-1112/02/6800–137$3.00/0

quitoes and through handling and consumption of infected livestock (Daubney *et al.*, 1931; Scott *et al.*, 1956; Davies, 1975). Most areas which experience RVF epizootics exhibit a prolonged dry season, and outbreaks occur when there is heavy and widespread rainfall (Davies *et al.*, 1985). For example, simultaneous outbreaks in Zimbabwe and Mozambique in 1969 (Valadao, 1969; Peters and Linthicum, 1994), South Africa and Namibia in 1975, and in Kenya at different times between 1950 and 1998 were related to widespread, persistent and above average rainfall following periods of extensive drought (Scott *et al.*, 1956; Peters and Linthicum, 1994; Linthicum *et al.*, 1999).

Remote Sensing of the Ecology of RVF

Since the early 1980s, there have been attempts to use remote sensing data to identify ecological conditions associated with RVF outbreaks in East Africa (Linthicum *et al.*, 1987). Most of the data that have been used in such studies are from measurements made by the Advanced Very High Resolution Radiometer (AVHRR) instrument aboard the National Oceanographic and Atmospheric Administration (NOAA) series of polar orbiting satellites. Measurements in the visible red and near infrared bands on this instrument are of specific relevance to ecology.

Plant canopies have a strong chlorophyll absorption in the red portion of the spectrum and a very high reflectance in the near infrared portion. This unique spectral response of vegetation makes it possible to differentiate vegetation from other surface materials remotely. The normalized difference vegetation index is derived from these measurements in the form

$$\mathrm{NDVI} = \frac{\rho_{\mathrm{nir}} - \rho_{\mathrm{red}}}{\rho_{\mathrm{nir}} + \rho_{\mathrm{red}}}$$

where ρ_{nir} and ρ_{red} and the surface reflectances in the near-infrared and red portions of the electromagnetic spectrum respectively (Tucker, 1979). Derived NDVI values range between −1 to +1, with values below zero indicating absence of vegetation and those above 0 showing increasing amounts of green vegetation. This index provides a robust measure of the presence and abundance of vegetation in a wide range of environmental conditions (Prince, 1991). NDVI has been found to be very useful in monitoring vegetation dynamics in semi-arid and arid areas where grasslands and savanna bushlands are the dominant vegetation types (Hiernaux and Prince, 1986; Prince and Tucker, 1986). This is primarily because semi-arid vegetation is very sensitive to variations in precipitation. Comparative data show that there is a near linear relationship between NDVI and precipitation in a range of semi-arid lands of Africa (Nicholson *et al.*, 1990; Tucker *et al.*, 1991). Precipitation and green vegetation dynamics are a major determinant of life cycles of animals and insects in semi-arid lands of Africa. Various research studies indicate a close relationship between the seasonal trace of green vegetation development (NDVI) with breeding and upsurge patterns of particular insect vectors including locusts and mosquitoes (Tucker *et al.*, 1985a; Tucker *et al.*, 1985b; Hielkema *et al.*, 1986; Linthicum *et al.*, 1987; Linthicum *et al.*, 1990; Hay *et al.*, 2000). Widespread heavy rains result in vegetation development, and provide a good environment for immature and adult mosquito vector populations to increase, significantly elevating the risk of RVF outbreaks (Linthicum *et al.*, 1983; Linthicum *et al.*, 1984).

Climatic Context of RVF Outbreak Patterns

Rainfall in semi-arid lands of Africa ranges between about 200 and 800 mm/yr. and exhibits large year-to-year variability, on the order of 20 to 30 percent or more of the average annual value (Rasmusson, 1988; Janowiak, 1988). Characteristics of rainfall variability patterns have been examined (Nicholson, 1980a; Nicholson, 1980b; Nicholson, 1986). There is a tendency for persistence of drought or above-normal rainfall periods with marked biennial characteristics over East Africa and southern Africa (Nicholson and Entekhabi, 1986). The Sahel region shows much longer, decadal-scale variability (Nicholson and Palao, 1993). Given the nearly linear relationship between rainfall and NDVI, it is thus possible to utilize NDVI to examine spatially and temporally, land surface patterns and impacts of drought or above normal rainfall in areas with limited rain gauge measurements. At the interannual time scale, the seesaw between wet and dry years has been linked to the El Niño/Southern Oscillation (ENSO) climate phenomenon that results from the changes in sea surface temperature gradients in the equatorial Pacific Ocean (Cane, 1983; Rasmusson and Wallace, 1983). Given the sheer size of the Pacific Ocean, changes in the sea surface temperatures (SSTs) in this region have an effect on global tropical circulation mechanisms. The occurrence of a warm (El Niño) or cold (La Niña) phase of ENSO leads to large-scale shifts in precipitation patterns across the global tropics and, as a consequence, pathogen and vector abundance (Linthicum *et al.*, 1999). Over Africa, there is a tendency for drought (wet) conditions over southern Africa during El Niño (La Niña) periods and the reverse conditions over East Africa. The signal of ENSO in vegetation has been detected by examining NDVI time series for Africa and elsewhere (Eastman and Fulk, 1993; Myneni *et al.*, 1995; Anyamba and Eastman, 1996). Given the spatially continuous nature of these data sets, the anomalous conditions resulting from ENSO-linked precipitation variability can be mapped (Anyamba *et al.*, 2001). Recently, it is has been shown that interannual variability in rainfall, SSTs, and NDVI coincide with historical RVF outbreak patterns in Kenya (Linthicum *et al.*, 1999). Above normal SSTs, both in region 3.4 of the equatorial eastern Pacific (NINO 3.4) and in the equatorial western Indian Ocean (WIO), lead to above normal and widespread precipitation and persistence of above normal NDVI over East Africa. The life cycle of mosquitoes that carry the RVF virus is coupled to such rainfall events, with thousands of mosquitoes emerging from *dambo* (shallow ground depression) environments following above normal rainfall (Linthicum *et al.*, 1983; Linthicum *et al.*, 1984). The close coupling between ENSO, rainfall, NDVI response patterns, and mosquito life cycle dynamics provides a basis for using NDVI time series measurements to map areas at risk from RVF.

Data and Analysis Methods

To identify areas at risk from RVF outbreaks, we considered several factors:

- The dynamics of mosquito species succession in flooded habitats (Linthicum, 1983; Linthicum, 1984).
- Based on previous studies using NDVI (Hiernaux and Justice, 1986; Nicholson *et al.*, 1990; Prince, 1991; Anyamba and Eastman, 1996)), we determined the ecosystem zones with a pronounced interannual variability signal where previous RVF outbreaks have occurred (Linthicum *et al.*, 1999).
- We evaluated the persistence in positive NDVI anomalies in these areas above some critical threshold during the climatological rainfall season.
- We selected for evaluation at-risk periods based on SST anomalies in the NINO 3.4 and WIO regions in order to identify El Niño and La Niña episodes.
- Periods of high positive (negative) departure in SSTs (NINO 3.4 and WIO) regions coincide with periods of above (below) normal rainfall and enhanced (depressed) NDVI in East Africa (southern Africa) and vice versa (Linthicum *et al.*, 1999; Anyamba *et al.*, 2001).

Based upon extensive experience concerning the relationship between NDVI and RVF transmission in various regions of Africa (Linthicum *et al.*, 1987; Davies *et al.*, 1992; Linthicum *et al.*, 1994), we assumed that persistence of positive NDVI anomalies (average greater than 0.1 NDVI units) for a period of three months (resulting from above normal and widespread rainfall)

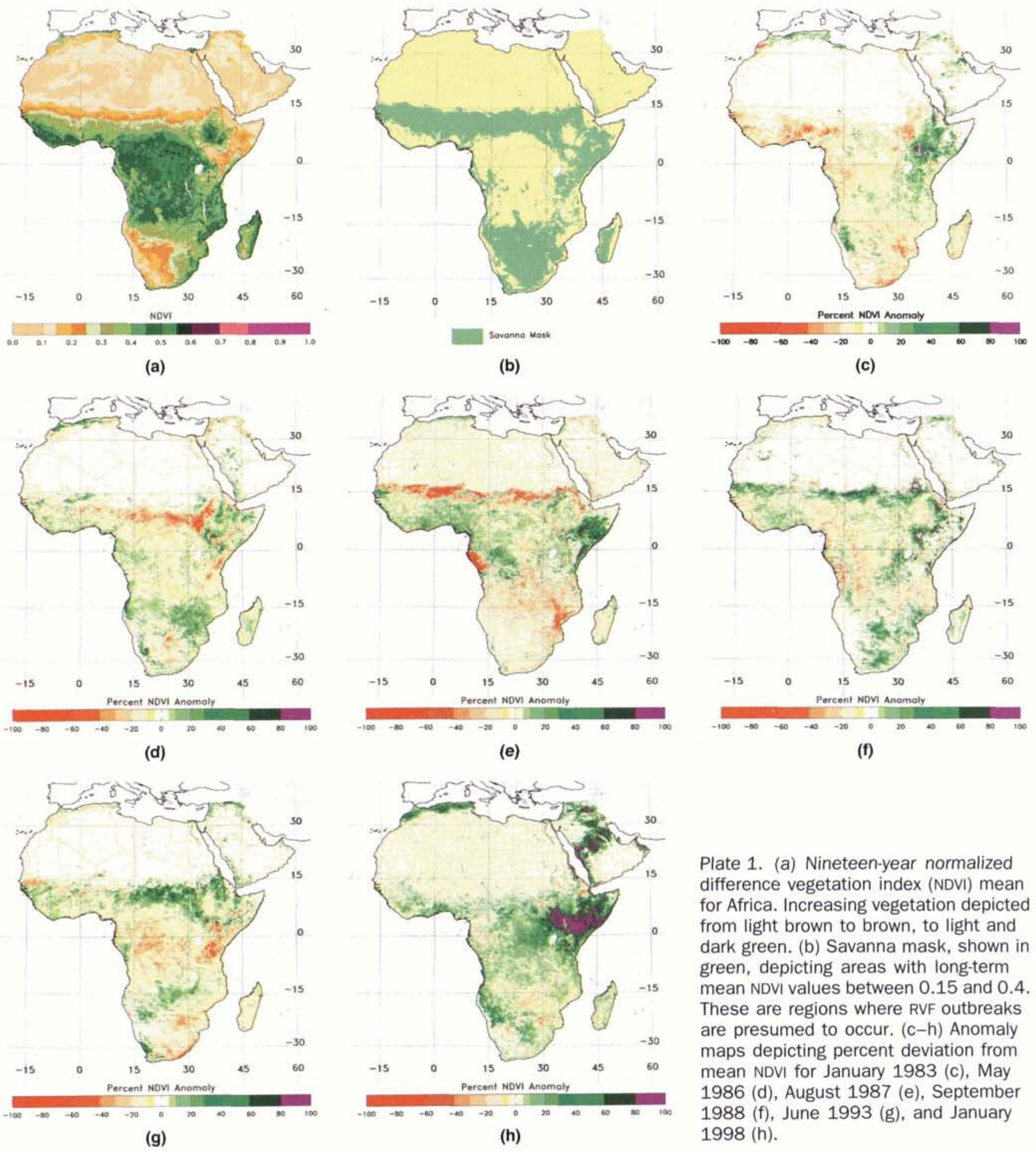

Plate 1. (a) *Nineteen-year normalized* difference vegetation index (NDVI) mean for Africa. Increasing vegetation depicted from light brown to brown, to light and dark green. (b) Savanna mask, shown in green, depicting areas with long-term mean NDVI values between 0.15 and 0.4. These are regions where RVF outbreaks are presumed to occur. (c–h) Anomaly maps depicting percent deviation from mean NDVI for January 1983 (c), May 1986 (d), August 1987 (e), September 1988 (f), June 1993 (g), and January 1998 (h).

would create the ecological conditions necessary for large-scale mosquito vector breeding and subsequent transmission of RVF virus to domestic animals and humans.

In order to identify areas at-risk to RVF outbreak, several procedures were implemented. We created a long-term NDVI climatology (at 8- by 8-km spatial resolution) to define the vegetation patterns for Africa for the period July 1981 through July 2000. This map defines for us the broad continental-scale vegetation zones from which to segregate between different vegetation cover types. This NDVI long-term mean map shown in Plate 1a is very similar to maps derived from classification of NDVI time series data by Tucker *et al.* (1985a; 1985b). Using a thresholding method, we define, based on the NDVI climatology map, semi-arid regions of Africa which correspond to regions with climatalogical mean values that range between 0.15 to 0.4 NDVI units (Plate 1b). This map identifies the savanna complexes of Africa, which are subject to extremes in interannual climate variability (Rasmusson, 1988). This mask includes those areas that receive between 200 and 800 mm/yr of rainfall. These are primarily the regions where RVF outbreaks have been described, especially in East Africa, southern Africa, and the Sahel region (Peters and Linthicum, 1994). We refer to this as the Savanna mask. The Savanna mask is specifically designed to omit tropical forest, desert, and some wet savanna regions (such as those seen in Zambia), and concentrate on areas likely to have RVF epizootics. In Zambia regular, persistent, and heavy rainfall tends to create a pattern of regular low-level RVF activity, and not large-scale epizootics (Davies *et al.*, 1992). Because of persistent RVF activity in Egypt since 1977, we have included the Nile River Valley and Delta region in the Savanna mask.

We calculated NDVI monthly anomalies to define the extremes in eco-climatic conditions from the long-term (1982–1999) monthly NDVI means as follows:

$$\mathrm{NDVI}_{\Delta} = \mathrm{NDVI} - \overline{\mathrm{NDVI}}$$

where the NDVI_{Δ} are the respective monthly anomalies, the NDVI are monthly values, and the $\overline{\mathrm{NDVI}}$ long-term monthly means, respectively.

Some examples of NDVI anomalies are shown in Plates 1c through 1h (shown here as percent departures from long-term means). We examined persistence in positive NDVI anomalies for selected periods defined by climatological seasons. For example, for East Africa, we examine the persistence in positive NDVI anomalies for the period September through November (the short rainy season denoted SON) when the ENSO-precipitation relationship is known to be most pronounced (Ropelewski and Halpert, 1987; Ogallo, 1988). Risk is defined based on persistence of positive NDVI anomalies for any given three-month period according to the following criteria:

(1) Areas must have positive anomalies above the noise level (greater than 0.025, NDVI) for three consecutive months. Expressed as anomalies, NDVI values over the desert areas fluctuate between plus and minus 0.025; therefore, we considered any variation greater or less than these values of real significance to ecological dynamics: i.e.,

$$\mathrm{NDVI}_{\Delta t} \geq +0.025 \text{ and } \mathrm{NDVI}_{\Delta t-1} \geq +0.025 \text{ and } \mathrm{NDVI}_{\Delta t-2} \geq +0.025.$$

(2) Persistently positive anomalies must have a three-month mean NDVI anomaly exceeding a threshold of 0.1 NDVI: i.e.,

$$\overline{\mathrm{NDVI}}_{\Delta(3mon)} > 0.1$$

where $\overline{\mathrm{NDVI}}_{\Delta(3mon)}$ is the average NDVI anomaly over the last three months (i.e., t, $t-1$, $t-2$; that is, current and two previous months): i.e.,

$$\overline{\mathrm{NDVI}}_{\Delta(3mon)} = \frac{\sum_{t}^{t-2} \mathrm{NDVI}_{\Delta t}}{3}.$$

All regions meeting these criteria within the Savanna mask are identified and mapped as areas potentially at risk for occurrence of RVF. This enables us to track the progression of the growing season because NDVI values increase with time above the noise level (in this case to $\pm$ 0.025) to values greater than 0.1 under anomalous climatic conditions as, for example, observed in East Africa in 1998/98 (Linthicum *et al.*, 1999).

We applied the above technique to NDVI anomaly data for both El Niño and La Niña periods identified by examining SST departure patterns in NINO 3.4 and WIO (1982/83, 1984/85, 1986/87, 1988/89, 1991/92, 1994/95, 1996/97, 1997/98, 1999/00) (Figure 1). We mapped all pixels that meet the above criteria and lie within the Savanna mask in red as areas at risk to RVF (Plate 2).

Finally, we generated frequency statistics on the number of RVF risk pixels identified for three regions: East Africa (10°S to 15°N, 30°E to 50°E), southern Africa (11°S to 30°S, 13°E to 50°E), and the Sahel (12°N to 18°N, 17°W to 30°E). The results are shown in Figure 2 by region for different periods to illustrate what periods showed the highest risk by area coverage. One-hundred sixty-four thousand eight-hundred fifty pixels, representing 10,550,400 km², are included in the Savanna mask.

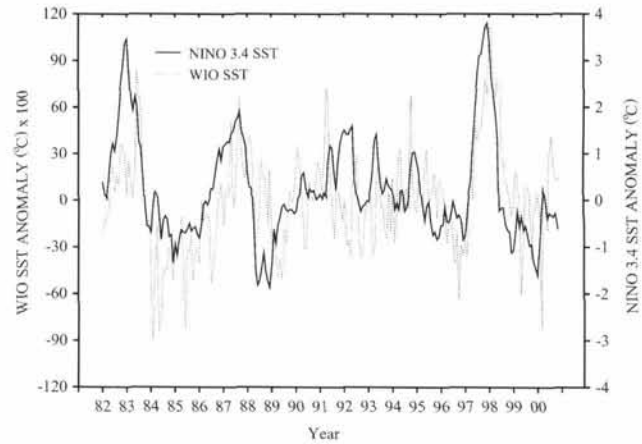

Figure 1. Equatorial Western Indian Ocean (WIO) and equatorial Eastern Pacific Ocean (NINO 3.4) sea surface temperature (SST) time series from 1982 through 2000. SSTs are depicted as positive or negative anomalies from long-term mean (=0°C). Values plotted are monthly anomalies, with the year designation indicating January of the respective year.

Results and Discussion

Risk maps were generated after applying procedures described above to NDVI anomaly time series data, and were interpreted in relation to interannual variability patterns in SST anomalies in the WIO and NINO 3.4 regions. RVF risk results are presented in binary images. Areas flagged as red within the Savanna mask represent risk for RVF for that period; areas shown in green are within the RVF endemic mask and show no risk. Other areas (shown in yellow), desert, and dense tropical forest were not included in this analysis (Plate 2).

During the 1982/83 period a warm ENSO event was manifest with a peak in SST anomalies in NINO 3.4 and WIO regions of +3.0° and +0.8°C, respectively (Figure 1). Positive NDVI anomalies persisted for several months covering most of the semi-arid lands of East Africa (Plate 1c). Areas that show risk are predominantly within the RVF endemic region of Kenya and northern Tanzania and extending north into the Rift region of Ethiopia (Plate 2a). Almost 5 percent of the pixels in the Savanna mask were flagged in East Africa at this time (Figure 2a). RVF activity was detected in Kenya around Nairobi during this period (Linthicum *et al.*, 1985). A mild cold event occurred during the 1984/85 period, with SST anomalies on the order of −1.0°C in the NINO 3.4 and −0.6°C the WIO region (Figure 1). Drought persisted over East Africa but greener than normal conditions were experienced over southeastern Africa. The identified area of risk is confined to the border region of Zimbabwe, South Africa, and Mozambique (not shown). A slight increase in flagged pixels was observed in southern Africa (Figure 2b). No other areas are identified over the continent during this period. Drought prevailed over most of the continent during the 1984–1985 period; it is therefore not surprising that potential RVF activity was limited. In addition, rainfall was not as widespread as would normally be expected over southern Africa

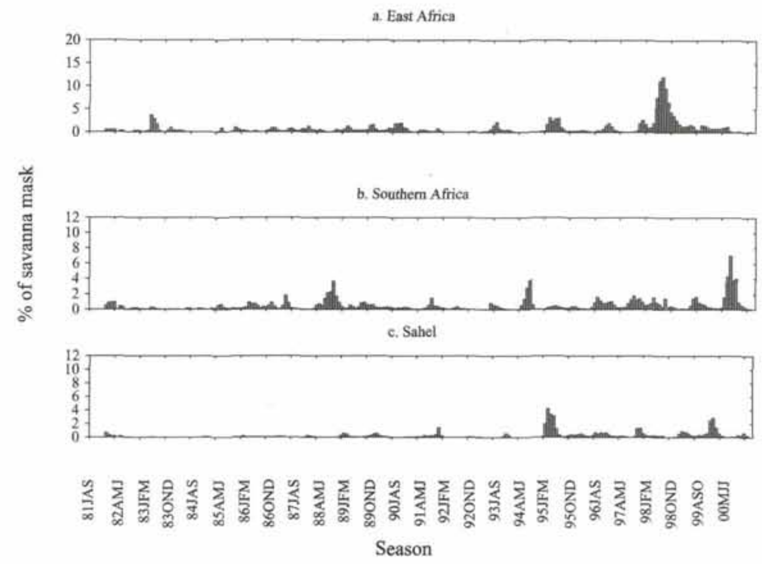

Figure 2. Percentage of pixels in the Savanna mask that were flagged as having a risk for RVF virus transmission in East Africa (a), southern Africa (b), and the Sahel Region (c). Data depicted for rolling three-month periods between July 1981 and July 2000 (i.e., 81JAS = July, August, September 1981).

during a La Niña episode (Nicholson and Entekhabi, 1986; Anyamba and Eastman, 1996). There was some suggestion of RVF epizootic activity in 1983 in Burkina Faso (Saluzzo *et al.*, 1984) and in 1985 in the Central African Republic (CAR) (Peters and Linthicum, 1994); however, during these periods there were no pixels flagged in the areas of interest (Figure 2c). We conclude that either there were no epizootics or no significant vegetation anomalies in Burkina Faso and the CAR, and/or the Savanna mask did not include areas involved in the epizootic in the CAR.

A change to warmer SST anomaly conditions (+2.0°C in NINO 3.4, +0.6°C in WIO) in 1986/87 resulted in a cluster of persistent positive NDVI anomalies above the threshold (0.1) for December 1986 to February 1987 in East Africa. Areas of RVF risk were limited to the Serengeti grassland system in Tanzania extending northward into the Lake Magadi region in southern Kenya (not shown). However, no RVF activity was reported in Kenya or Tanzania during this period. In southern Africa, significantly elevated RVF activity was detected in Zambia during the 1985–1986 period, as shown by above normal NDVI (Plate 1d) and flagged pixels for the period April through June 1986 (Plate 2b) (Davies *et al.*, 1992). Very few or no flagged pixels were identified in Zambia during periods of repeated low-level RVF activity from 1982 through 1985, although consistently elevated NDVI values have been previously documented (Davies *et al.*, 1992).

Flagged pixels were observed in the Ferlo Region of Senegal from August through October 1987, just prior to the RVF epizootic that occurred just to the north in Senegal and Mauritania along the Senegal River in December 1987 (Plates 1e and 2c) (Digoutte and Peters, 1989). Part of the Senegal River itself was not included in the Savanna mask because it occurs in a desert area, but previous observations have documented elevated NDVI values along the river just prior to and during the outbreak in 1987 (Linthicum *et al.*, 1994). Warmer SST conditions persisted in 1988/89 for the WIO region while the NINO 3.4 switched to cold conditions (Figure 1). Positive NDVI anomalies persisted in southern Africa and East Africa (Plate 1f). We identified isolated areas of potential RVF risk in northwest Kenya extending to the central Rift Valley region (around Lakes Nakuru and Naivasha) of Kenya (Plate 2d) and in southern Africa (Free State Region of South Africa, eastern and central Botswana, and northwestern Ovamboland region of Namibia). Localized RVF activity was detected in the area around Lake Naivasha, Kenya during this period (Logan *et al.*, 1991; Logan *et al.*, 1992). An increase in the percentage of flagged pixels in 1988/1989 is seen in eastern and southern Africa (Figures 2a and 2b). This may be in part a result of slight but persistent above normal SSTs in the WIO region (+0.3 to +0.6°C) which resulted in above normal rainfall for the period 1988–89 in East Africa (Linthicum *et al.*, unpublished observations, 1989), although the eastern Pacific was colder than normal.

An RVF epizootic occurred in cattle in Madagascar on the eastern coastal plain in 1990 and in the highlands in 1991(Morvan *et al.*, 1991; Morvan *et al.*, 1992), and we detected some flagged pixels throughout Madagascar in the period December 1989 through February 1990 just prior to the start of the outbreak (Plate 2e). This epizootic occurred in an area of primary and deforested rain forest with a high annual rainfall (2,600 to 3,200 mm/year). During the mature phase of the 1991/92 warm event, there were no areas of persistent NDVI anomalies identified within the RVF endemic region over the whole continent except for a very restricted area in extreme southwestern Angola (not shown). Although 1991/92 was a warm ENSO event year, both East Africa and southern Africa experienced drought conditions (not shown). The expected above normal rainfall and positive NDVI anomalies in East Africa were not manifest during the short (October through December 1991) or the long rainy season (March through June, 1992). In part, we attribute this to colder than normal SST in the WIO region unlike during other warm ENSO events (Figure 1). RVF risk identified during this period was only limited to southwestern Angola. This is not entirely unexpected because the southern Africa region seems to show different spatial ENSO response patterns from one

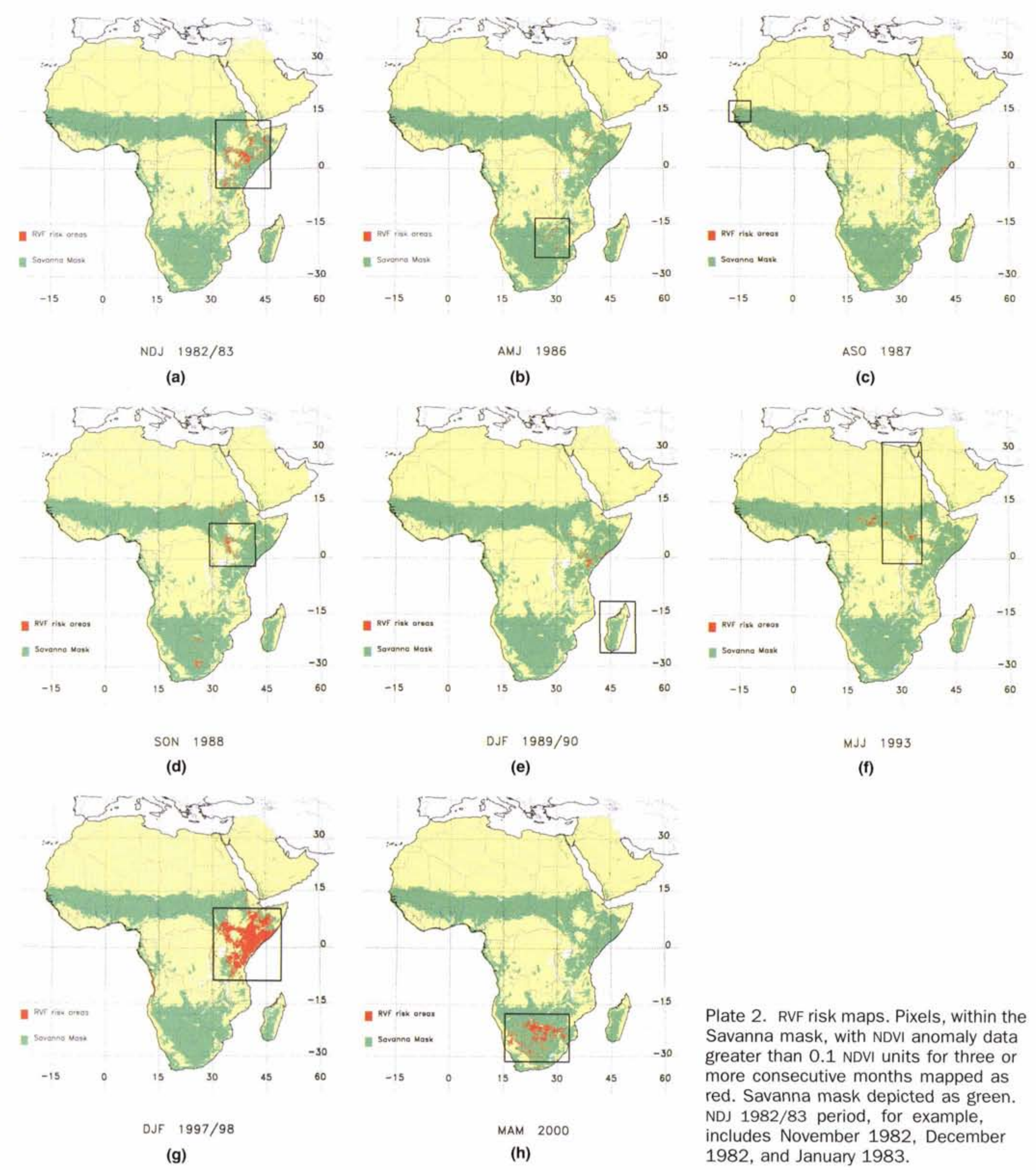

Plate 2. RVF risk maps. Pixels, within the Savanna mask, with NDVI anomaly data greater than 0.1 NDVI units for three or more consecutive months mapped as red. Savanna mask depicted as green. NDJ 1982/83 period, for example, includes November 1982, December 1982, and January 1983.

event to another (Eastman and Anyamba, 1996). RVF reemerged in Egypt in May 1993, possibly representing a reintroduction of the virus (Arthur *et al.*, 1993). We observed flagged pixels along the Nile between May and July 1993 (Plate 2f). Interestingly, there was an almost simultaneous positive NDVI anomaly (Plate 1g) and flagged pixels (Plate 2f) in southern Sudan at the headwaters of the Nile River, providing some evidence that the source of the RVF outbreak in Egypt may have originated to the south in Sudan.

RVF infected sheep, cattle, and mosquitoes were detected in 1993 in Senegal, although we did not observe any flagged pixels (Fontenille *et al.*, 1998). For the whole of the Sahel, clusters of potential RVF risk areas were identified across a region stretching from Senegal in the west to Sudan and the Turkana region of Kenya in the east during the period July through November 1994 (not shown). The June through October 1994 period was the wettest in the Sahel since 1967 (Halpert *et al.*, 1995). The resulting local flooding and elevated NDVI (not shown) over the region may have created conditions necessary for an RVF outbreak; however, no RVF activity was detected. The mild warm ENSO event, which peaked in January 1995 (SST of +2.0°C in NINO 3.4 and +0.6°C in WIO; Figure 1), produced drought conditions over southern Africa and above normal NDVI in isolated areas of East Africa (particularly in Kenya). We identify areas of potential RVF risk in isolated areas of semi-arid Kenya, Somalia, and southern Senegal during this period (not shown), but no RVF activity was detected.

Colder than normal SST conditions in the eastern Pacific and the WIO region prevailed during the period 1996/97 (Figure 1). NDVI was below normal in Kenya and Tanzania but above normal over southern Africa (not shown). We identified potential outbreak areas in northern Namibia through central Botswana to southern Zimbabwe for the growing season November 1996 through May 1997 (not shown). In addition, southern Sudan shows a number of areas flagged as potential risk to RVF.

SST conditions in both WIO and NINO 3.4 started to warm in May 1997, reaching a peak of 1.2°C (WIO) and 4.0°C (NINO 3.4) above normal in January and February 1998 (Figure 1). This warm ENSO event has been described as the strongest in this century (McPhaden, 1999). Large areas of East Africa received widespread and heavy rainfall during the short rains growing season (September through November, 1997) extending into the dry season (December 1997 through February 1998) (Birkett *et al.*, 1999). Elevated NDVI values dominated the semi-arid areas of East Africa, exceeding normal levels by 60 to 100 percent for several months (Plate 1h). As a result, there was a significantly increased risk for RVF outbreaks over a wide area including Kenya, Somalia, Tanzania, and parts of Ethiopia. The percentage of flagged pixels exceeded 5 percent of the Savanna mask for six consecutive months (Figure 2a). During this period, the largest RVF outbreak in the last 20 years occurred over a large geographic area (CDC, 1998). We identified an extensive area of East Africa at risk to RVF during this period (Plate 2g), which coincided closely with the geographic distribution of published case data (CDC, 1998). The number of flagged pixels in East Africa exceeded 20,000 (1,280,000 km^2), a 19-year peak (Figure 2a). Extensive warming of SST in the Pacific and WIO during the 1997/98 period gave way to cooling during the 1999/2000 period. This period was marked by above normal rainfall and extensive flooding in southern Africa and severe drought conditions in East Africa (not shown). A moving window analysis for this period identifies potential RVF outbreak areas in Namibia, Botswana, northern South Africa, and southern Zimbabwe (Plate 2h), although no RVF activity was detected.

Analysis and results from this study illustrate that large area monitoring of ecoclimatic conditions associated with disease outbreaks can be accomplished using polar orbiting satellite measurements. The ability to monitor rapidly changing ecological conditions can be an important tool for public health disease surveillance. The analysis carried out in this study illustrates that such proxy measurements of ecological conditions (NDVI) can help identify areas at risk to specific types of disease (in this case, RVF) whose outbreak is related to anomalous climate conditions. However, for this to be more useful, we need to have a more robust understanding of the biology and interaction between the vector, environment, and climate.

During the period from July 1981 to July 2000, we were able to retrospectively detect each of the three RVF outbreaks in East Africa, and quantify the geographic expanse based upon the number of pixels flagged as described above. In the Sahel region, we were able to detect the largest RVF outbreak in Senegal and Mauritania, but failed to detect significantly lesser RVF activity in Senegal (1993), Burkina Faso (1983), and the CAR (1985). Attempts to alter the spatial extent of the Savanna mask or the sensitivity of NDVI algorithm failed to achieve a better ability to predict RVF risk for small outbreaks in the Sahel region. Because we primarily based our methodology on what is known about the ecology of RVF transmission in East Africa, we conclude that differences in the ecology of the Sahel and/or unknown differences in the ecology of the virus prevent us from detecting small RVF outbreaks. Refinement may be possible when the ecology of RVF in Central and West Africa are better understood, and we can refine the thresholding criteria. In southern Africa, we detected elevated RVF activity in Zambia but failed to detect consistent low-level activity in previous years. Attempts to better define the Savanna mask in Zambia failed to improve our ability to detect small RVF outbreaks. We also successfully detected the start of the RVF epizootic in Madagascar in 1990. Both Zambia and the eastern coastal plain of Madagascar receive regular and consistent heavy rainfall that makes detection of anomalous vegetation conditions problematic. Regular and consistent heavy rainfall appears to lead to regular and consistent low-level RVF activity which we may not be able to detect with the methods described here (Davies *et al.*, 1992); however, slightly elevated RVF activity, above the background activity, in both Zimbabwe and Madagascar was detected in our risk maps.

What we have attempted to do here is to develop a profile of the likely spatial pattern of RVF outbreaks dependent on the population dynamics of vector mosquitoes and the occurrence of anomalous climatic conditions (ENSO), and some subjective time delay factor to identify areas at risk. The maps we derive are informative in the sense that, for the different periods analyzed, we clearly pick out a number of areas where outbreaks have or may have occurred in the past. In doing so, we may have reconstructed the likely historical patterns of RVF outbreaks. In addition, this type of mapping may provide public health authorities with first-level information about where to target disease surveillance teams, thus reducing the cost of disease surveillance over large areas (Myers *et al.*, 2000). Curiously, we also identify teleconnection patterns in areas at risk to RVF between East Africa and southern Africa that follow the inverse response patterns to ENSO between the two regions (Ropelewski and Halpert, 1987). Furthermore, we also recognize the importance of the state of the WIO region SST for RVF outbreak risk in East Africa as suggested in Linthicum *et al.* (1999). For example, we do not identify any areas in East Africa at risk to RVF during the 1991/92 ENSO warm event. Although the eastern Pacific was warmer than normal, the WIO region did not warm up as in any other number of warm events during the 20-year period; as a result, East Africa experienced drought conditions. This may indicate that a warmer than normal WIO SST is a necessary condition for RVF outbreak risk in eastern Africa, because this drives monsoon systems that bring rainfall to this region.

Acknowledgments

The results presented in this paper are part of collaborative research between NASA's Goddard Space Flight Center—Earth Sciences Directorate's Human Health Initiative and the Department of Defense—Global Emerging Infections System, Walter Reed Army Institute for Research. A. Anyamba was supported through USRA NAS5-98181 and through GEST under NASA/GSFC Cooperative Agreement with UMBC, NCC5-494.

References

Anyamba, A., and J.R. Eastman, 1996. Interannual variability of NDVI over Africa and its relationship to El Niño/Southern Oscillation, *International Journal of Remote Sensing*, 17:2533–2548.

Anyamba, A., C.J. Tucker, and J.R. Eastman, 2001. NDVI anomaly patterns over Africa during the 1997/98 warm ENSO event, *International Journal of Remote Sensing*, 10:1847–1859.

Arthur, R.R., M.S. El-Sharkawy, S.E. Cope, B.A. Butros, S. Oun, J.C. Morrill, R.E. Shope, R.G. Hibbs, M.A. Darwish, and I.Z.E. Imam, 1993. Recurrence of Rift Valley fever in Egypt, *Lancet*, 342: 1149–1150.

Birkett, C., R. Murtugudde, and T. Allan, 1999. Indian Ocean climate event brings floods to East Africa's lakes and the Sudd Marsh, *Geophysical Research Letters*, 26:1031–1034.

Cane, M.A., 1983. Oceanographic events during El Niño, *Science*, 222:77–90.

Centers for Disease Control (CDC), 1998. Rift Valley Fever: East Africa, 1997–1998, *Morbidity and Mortality Weekly Report*, 47:261–264.

Daubney, R., J.R. Hudson, and P.C. Garnham, 1931. Enzootic hepatitis or Rift Valley fever. An undescribed virus disease of sheep, cattle and man from East Africa, *Journal of Patholology and Bacteriology*, 34:545–579.

Davies, F.G., 1975. Observations on the epidemiology of Rift Valley Fever in Kenya, *Journal of Hygiene*, 75:219–230.

Davies, F.G., K.J. Linthicum, and A.D. James, 1985. Rainfall and epizootic Rift Valley fever, *Bulletin of the World Health Organization*, 63:941–943.

Davies, F.G., E. Kileulu, K.J. Linthicum, and R.G. Pegram, 1992. Patterns of Rift Valley fever activity in Zambia, *Epidemiology and Infections*, 108:185–191.

Digoutte, J.P., and C.J. Peters, 1989. General aspects of the 1987 Rift Valley fever epidemic in Mauritania, *Research in Virology*, 140: 27–30.

Eastman, J.R., and M. Fulk, 1993. Long sequence time-series evaluation using standardized principal components, *Photogrammetric Engineering & Remote Sensing*, 59:991–996.

Eastman, J.R., and A. Anyamba, 1996. Proto-typical patterns of ENSO related drought and drought-precursors in southern Africa, *Pecora Symposium Proceedings*, 20–22 August. Sioux Falls, South Dakota, .

Fontenille, D., M. Traore-Lamizana, M. Diallo, J. Thonnon, J.P. Digoutte, and H.G. Zeller, 1998. New vectors of Rift Valley fever in West Africa, *Emerging Infectious Diseases*, 4:289–293.

Hay, S.I., J.A. Omumbo, M.H. Craig, and R.W. Snow, 2000. Earth observation, geographic information systems and plasmodium falciparum malaria in sub-Saharan Africa, *Advances in Parasitology*, 47:173–215.

Hiernaux, P.H.Y., and C.O. Justice, 1986. Suivi du development vegetal au cours de l'ete 1984 dans le Sahel Malien, *International Journal of Remote Sensing*, 7:1515–1532.

Hielkema, J.U., J. Roffey, and C.J. Tucker, 1986. Assessment of ecological conditions associated with the 1980/1981-desert locust plague upsurge in West Africa using environmental satellite data, *International Journal of Remote Sensing*, 7:1609–1622.

Janowiak, J.E., 1988. An investigation of interannual rainfall variability in Africa, *Journal of Climate*, 1:240–255.

Linthicum, K.J., F.G. Davies, C.L. Bailey, and A. Kairo, 1983. A. Mosquito species succession dambo in an East African forest, *Mosquito News*, 43:464–470.

———, 1984. Mosquito species encountered in a flooded grassland dambo in Kenya, *Mosquito News*, 44:228–232.

Linthicum, K.J., F.G. Davies, A. Kairo, and C.L. Bailey, 1985. Rift Valley fever virus (family Bunyaviridae, genus *Phlebovirus*): Isolations from Diptera collected during an interepizootic period in Kenya, *Journal of Hygiene*, 95:197–209.

Linthicum, K.J., C.L. Bailey, F.G. Davies, and C.J. Tucker, 1987. Detection of Rift Valley fever viral activity in Kenya by satellite remote sensing imagery, *Science*, 235:1656–1659.

Linthicum, K.J., C.L. Bailey, C.J. Tucker, K.D. Mitchell, T.M. Logan, F.G. Davies, C.W. Kamau, P.C. Thande, and J.N. Wagateh, 1990. Application of polar-orbiting satellite data to detect Rift Valley fever vector mosquito habitats in Kenya, *Medical and Veterinary Entomology*, 4:433–438.

Linthicum, K.J., C.L. Bailey, C.J. Tucker, S.W. Gordon, T.M. Logan, C.J. Peters, and J.P. Digoutte, 1994. Observations with NOAA and SPOT satellites on the effect of man-made alterations in the ecology of the Senegal River basin in Mauritania on Rift Valley fever virus transmission, *Sistema Terra*, 3:44–47.

Linthicum, K.J., A. Anyamba, C.J. Tucker, P.W. Kelley, M.F. Myers, and C.J. Peters, 1999. Southern Oscillation Index, sea surface temperature and satellite vegetation index indicators to forecast Rift Valley fever epizootics/epidemics in Kenya, *Science*, 285(5426):397–400.

Logan, T.M., K.J. Linthicum, F.G. Davies, Y.S. Binepal, and C.R. Roberts, 1991. Isolation of Rift Valley fever virus from mosquitoes collected during an outbreak in domestic animals in Kenya, *Journal of Medical Entomology*, 28:293–295.

Logan, T.M., F.G. Davies, K.J. Linthicum, and T.G. Ksiazek, 1992. Rift Valley fever antibody in human sera collected after an outbreak in domestic animals in Kenya, *Transactions of the Royal Society of Tropical Medicine and Hygiene*, 86:202–203.

McIntosh, B.M., and P.G. Jupp, 1981. Epidemiological aspects of Rift Valley fever in South Africa with references to vectors, *Contributions to Epidemiology and Biostatics*, 3:92–99.

McPhaden, M.J., 1999. Genesis and evolution of the 1997–98 El Niño, *Science*, 283:950–954.

Megan, J.M., and C.L. Bailey, 1989. Rift Valley fever, *The Arboviruses: Epidemiology and Ecology* (T.P. Monath, editor), Vol. IV, CRC Press Inc., Boca Raton, Florida, pp. 51–76.

Morvan, J., J.F. Saluzzo, D. Fontenille, P.E. Rollin, and P. Coulanges, 1991. Rift Valley fever on the east coast of Madagascar, *Research in Virology*, 142:475–482.

Morvan, J., P.E. Rollin, S. Laventure, and J. Roux, 1992. Duration of immunoglobulin M antibodies against Rift Valley fever virus in cattle after natural infection, *Transactions of the Royal Society of Tropical Medicine and Hygiene*, 86:675.

Myneni, R.B., S.O. Los, and C.J. Tucker, 1995. Satellite-based identification of linked vegetation index and sea surface temperature anomaly areas from 1982–1990 for Africa, Australia and South America, *Geophysical Research Letters*, 23:729–732.

Myers, M.F., D.J. Rogers, J. Cox, A. Flahault, and S.I. Hay, 2000. Forecasting disease risk for increased epidemic preparedness in public health, *Advances in Parasitology*, 47:309–330.

Nicholson, S.E., 1980a. The nature of rainfall fluctuations in subtropical West Africa, *Monthly Weather Review*, 108:473–487.

———, 1980b. Sub-Saharan rainfall in the years 1976–1980: Evidence of continued drought, *Monthly Weather Review*, 111:1646–1654.

———, 1986. The spatial coherence of African rainfall anomalies: Interhemispheric teleconnections, *Journal of Climate and Applied Meteorology*, 25:1365–1381.

Nicholson, S.E., M.L. Davenport, and A.R. Malo, 1990. A comparison of vegetation response to rainfall in the Sahel and East Africa using Normalized Difference Vegetation Index from NOAA-AVHRR, *Climate Change*, 17:209–241.

Nicholson, S.E., and D. Entekhabi, 1986. The quasi-periodic behavior of rainfall variability in Africa and its relationship to the Southern Oscillation, *Archive Fur Meteorologie Geophysik und Bioklimatologie. A*, 34:311–348.

Nicholson, S.E., and I.M. Palao, 1993. A re-evaluation of rainfall variability in the Sahel, Part I. Characteristics of rainfall fluctuations, *International Journal of Climatology*, 13:371–389

Ogallo, L.J., 1988. Relationships between seasonal rainfall in East Africa and the Southern Oscillation, *International Journal of Climatology*, 8:31–43.

Peters, J.M., and J.M. Meegan, 1981. Rift Valley fever, *Handbook of Zoonoses* (G.B. Beran, editor), CRC Press Inc., Boca Raton, Florida, p. 403.

Peters, C.J., and K.J. Linthicum, 1994. Rift Valley fever, *Handbook of Zoonoses* (G.B. Beran, editor), CRC Press Inc., Boca Raton, Florida, pp. 125–138.

Prince, S.D., 1991. Satellite remote sensing of primary production: Comparison of results of Sahelian grasslands 1981–1988, *International Journal of Remote* Sensing, 12:1301–1312.

Prince, S.D., and C.J. Tucker, 1986. Satellite remote sensing of rangelands in Botswana. II. NOAA-AVHRR and herbaceous vegetation, *International Journal of Remote Sensing*, 7:1555–1570.

Rasmusson, E.M., 1988. Global climate change and variability: effects on drought and desertification in Africa, *Drought and Hunger in Africa* (G.H. Glantz, editor), Cambridge University Press, New York, N.Y., pp. 4–36.

Rasmusson, E.M., and J.M. Wallace, 1983. Meteorological aspects of El Niño/Southern Oscillation, *Science*, 222:1195–1202.

Ropelewski, C.F., and M.S. Halpert, 1987. Global and regional scale precipitation patterns associated with El Niño/Southern Oscillation, *Monthly Weather Review*, 115:1606–1626.

Saluzzo, J.F., J.P. Digoutte, M. Cornet, D. Baudon, J. Roux, and V. Robert, 1984. Isolation of Crimean-Congo haemorrhagic fever and Rift Valley fever viruses in Upper Volta, *Lancet*, 1(8387):1179.

Scott, G.R., W. Weddell, and D. Reid, 1956. Preliminary finding on the prevalence of Rift Valley in Kenya cattle, *Bulletin of Epizootic Diseases of Africa*, 4:17–25.

Swanepoel, R., 1981. Observations on Rift Valley fever in Zimbabwe, *Contributions to Epidemiology and Biostatistics*, 3:83–91.

Tucker, C.J., 1979. Red and photographic infrared linear combinations for monitoring vegetation, *Remote Sensing of Environment*, 8:127–150.

Tucker, C.J., J.U. Hielkema, and J. Roffey, 1985a. The potential of satellite remote sensing of ecological conditions for survey and forecasting desert-locust activity, *International Journal of Remote Sensing*, 6:127–138.

Tucker, C.J., J.R.G. Townshend, and T.E. Goff, 1985b. African Land-Cover classification using satellite data, *Science*, 227:369–375.

Tucker, C.J., H.E. Dregne, and W.W. Newcomb, 1991. Expansion and contraction of the Sahara Desert from 1980–1990, *Science*, 253:299–301

Valadao, F.G., 1969. Nota previa sobre a occrrencia du uma noa doenca em Mocambique—a febre du Vale de Rift, *Veterinary Mocambicana*, 2:13.

Wilson, M.L., L.E. Chapman, D.B. Hall, E.A. Dykstra, K. Ba, H.G. Zeller, M. Traore-Lamizana, J.P. Hervy, K.J. Linthicum, and C.J. Peters, 1994. Rift Valley fever in rural northern Senegal: Human risk factors and potential vectors, *American Journal of Tropical Medicine and Hygiene*, 50:663–675.

WHO (World Health Organization), 2000. Control of first Rift Valley fever outbreak outside Africa is under way, *Press Release WHO/62*, 29 September 2000.